ARTICLE

Dye-Sensitized Solar Cells Employing a Single Film of Mesoporous TiO_2 Beads Achieve Power Conversion Efficiencies Over 10%

Frédéric Sauvage,[†] Dehong Chen,[‡] Pascal Comte,[†] Fuzhi Huang,[⊥] Leo-Philipp Heiniger,[†] Yi-Bing Cheng,[⊥,*] Rachel A. Caruso,[‡,§,*] and Michael Graetzel[†,*]

[†]Laboratoire de Photonique et Interfaces, Institut des Sciences et Ingénieurie Chimiques, Ecole Polytechnique Fédérale de Lausanne (EPFL), Station 6, CH-1015, Lausanne, Switzerland, [‡]The University of Melbourne, PFPC, School of Chemistry, 3010 Melbourne, Victoria, Australia, [§]CSIRO Materials Science and Engineering, Private Bag 33, 3169 Clayton South, Victoria, Australia, and [⊥]Monash University, Department of Materials Engineering, 3800 Melbourne, Victoria, Australia

ABSTRACT Dye-sensitized solar cells employing mesoporous TiO_2 beads have demonstrated longer electron diffusion lengths and extended electron lifetimes over Degussa P25 titania electrodes due to the well interconnected, densely packed nanocrystalline TiO_2 particles inside the beads. Careful selection of the dye to match the dye photon absorption characteristics with the light scattering properties of the beads have improved the light harvesting and conversion efficiency of the bead electrode in the dye-sensitized solar cell. This has resulted in a solar to electric power conversion efficiency (PCE) of greater than 10% (10.6% for Ru(II)-based dye C101 and 10.7% using C106) for the first time using a single screen-printed titania layer cell construction (that is, without an additional scattering layer).

KEYWORDS: TiO_2 · beads · C101 dye · dye-sensitized solar cells · DSC

Titanium dioxide is one of the most investigated inorganic semiconductor oxide materials found in today's literature due to its opto-electronic properties which make it appropriate for a variety of applications ranging from photocatalysis,[1] photochromism,[2] Li-ion batteries,[3] and chemical and gas sensors,[4,5] to use as the photoanode for dye-sensitized solar cells (DSC).[6] The DSC is unique in that it is the only photovoltaic device that achieves the separation of light absorption and charge carrier transport during the photoelectric conversion process, mimicking the photosynthesis found in green leaves. The performance of the cell, measured in terms of power conversion efficiency (PCE), depends closely on the light harvesting capacities of the dye adsorbed on the TiO_2 surface, the transport of the photoinjected electrons through the semiconductor electrode, and the dynamics of interfacial losses resulting from the possible recombination of the electrons with either the oxidized dye (S^+) or the oxidized electrolyte species produced upon regeneration of the oxidized sensitizer (such as I_3^- found in traditionally used electrolyte systems).

When the dye molecules capture the photons and inject excited electrons to the conduction band of TiO_2, the diffusion of the electrons and the lifetime of the electrons become vital. Fast electron diffusion is necessary for a high performance DSC. In a traditional nanocrystalline TiO_2 electrode film, the TiO_2 particles are not densely packed, therefore the length of the electron path to the conducting substrate is longer, increasing the chance of interfacial losses. Nanorods and nanotubes of TiO_2 vertically aligned on the transparent conducting electrode (TCO) have been synthesized to address this issue.[7,8] The electrons can easily pass along the nanorods to the TCO. However, the low surface area of the nanorods has prevented high efficiencies from being achieved. A densely packed mesoporous TiO_2 film was prepared *via* a self-assembly process by Lancelle-Beltran *et al.*, but the limited thickness of the film and its high transparency hamper the cell performance.[9] A very well interconnected TiO_2 nanocrystalline film with a strong scattering ability would produce a highly efficient DSC.

We report herein on the use of a single titania layer composed of mesoporous submicrometer sized beads in DSC reaching a high power PCE of over 10%.[10,11] Figure 1a illustrates the morphology of the TiO_2 beads in the screen-printed film for this study. The particles are relatively monodisperse, exhibiting a spherical morphology with a di-

*Address correspondence to yibing.cheng@eng.monash.edu.au, rcaruso@unimelb.edu.au, michael.graetzel@epfl.ch.

Received for review May 12, 2010 and accepted July 15, 2010.

Published online July 22, 2010. 10.1021/nn1010396

ameter of approximately 830 nm. The large size of the beads gives the film the ability to scatter light, according to the Mie-theory.[12] Normally, to introduce such a light scattering effect, a scattering layer comprising particles 400 nm in size is coated on top of the nanocrystalline TiO_2 layer. This double-layer configuration makes the fabrication process more complex and potentially increases the cost of manufacture. In addition, the mesoporous structure of the beads still provides sufficient surface area for the dye attachment. BET analysis indicates a surface area of 89 m^2/g and a mean pore size of *ca.* 23 nm calculated from N_2 adsorption data. The TEM image in Figure 1b shows the spheres are mesoporous to the core and consequently the titania particles within the beads remain easily accessible for chemisorption of the dye. High resolution TEM, Figure 1c,d, of the ultramicrotomed beads shows the TiO_2 nanocrystals inside the beads were densely packed with every grain having multiple contacts to neighboring grains. The image in Figure 1d presents evidence of intergrowth between the anatase crystals. Such intergrowth would decrease the negative effects of electron grain boundary crossing and is expected to be responsible for the extended electron lifetime and reduced recombination within the bead electrode structures (discussed later).

To determine cell efficiency, electron lifetime, and diffusion coefficient, cells were constructed with mesoporous TiO_2 beads and commercial Degussa P25 titania nanoparticles as a comparison. Here the heteroleptic Ru(II) thiophene-based complex, Na-*cis*-Ru(4,4′-(5-hexylthiophen-2-yl)-2,2′-bipyridine)(4-carboxylic-acid-4′-carboxylate-2,2′-bipyridine) (thiocyanate)$_2$, coded C101, was used as the sensitizer. Compared to the actual benchmark N719 or Z907 complexes, the heteroleptic C-dyes present certain advantages: A greater molar extinction coefficient ($\varepsilon_{C101} = 17500$ L/mol.cm) and a red-shifted metal-to-ligand charge transfer absorption ($\lambda_{C101} = 547$ nm) resulting from the extended π conjugation in the ancillary ligand.[13,14] As a result, C101 shows stronger absorption in the range of 600−800 nm than N719 or Z907.[13] The diffuse reflectance characteristics of the 12 μm thick mesoscopic film[10] were matched with the absorption properties of C101. The light scattered by the beads would be more effectively used by the C101 dye. Insight into the electron transport and recombination dynamics of these beads was gained by utilization of photovoltage and photocurrent transient techniques. For the first time PCEs exceeding the 10% threshold were obtained utilizing single titania layer films composed of these TiO_2 beads owing to their unique morphology, that is, a 10.6% efficiency (η) under standard air mass (AM) 1.5 global sunlight exposure of 1000 W/m^2 intensity using C101 ruthenium sensitizers. By contrast, a similar electrode sensitized with the N719 dye gave 8.3% PCE, thus underlining the important step forward achieved by the combination of

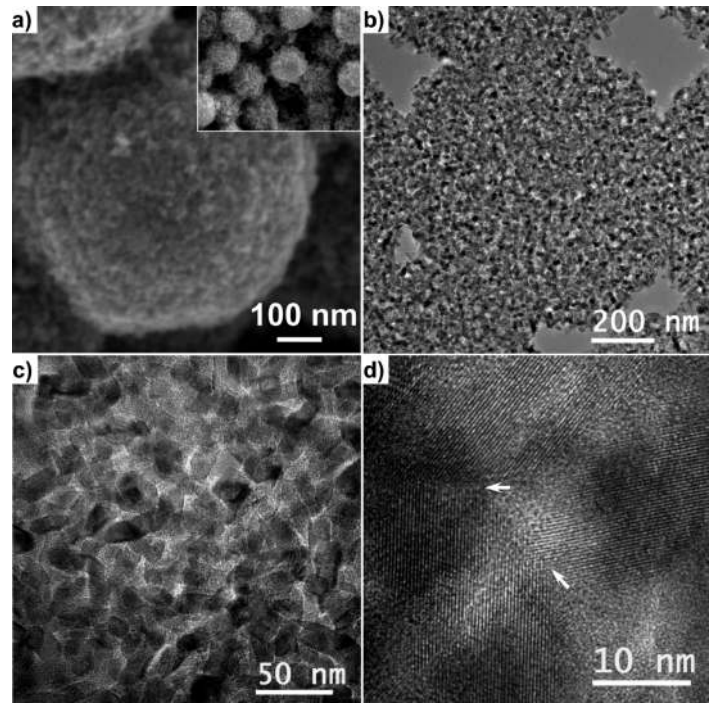

Figure 1. (a) Scanning electron microscope micrograph of the screen-printed film composed of TiO_2 porous beads; (b, c) TEM images of the ultramicrotomed titania bead; and (d) HRTEM image of the intergrowth of the anatase crystals, as indicated by the white arrows, within the titania bead.

beads and C101 dye (Supporting Information, Figure S1).

The (*J*−*V*) properties of the cells composed of P25 or beads sensitized with C101 are shown in Figure 2, at 1 equiv sunlight intensity, both before and after $TiCl_4$ post-treatment. With no $TiCl_4$ post-treatment, a 12 μm thick layer of sensitized beads exhibits a remarkable 9.1% conversion efficiency. As previously experienced by the scientific community when using standard mesoporous films, $TiCl_4$ post-treatment

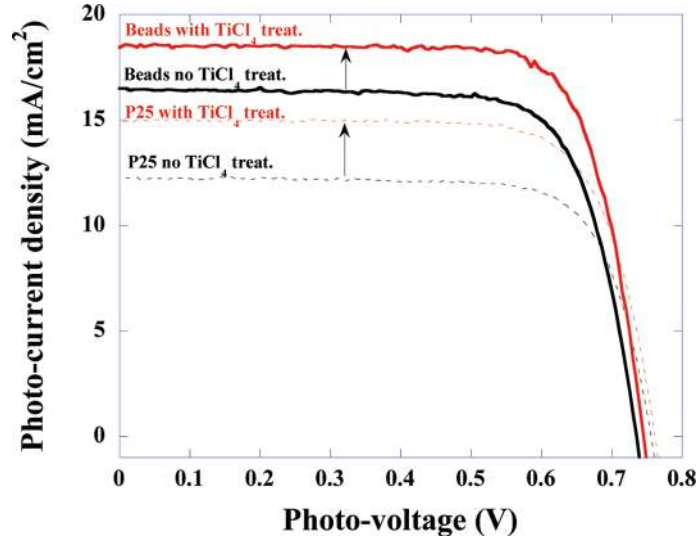

Figure 2. (*J*−*V*) characteristics recorded at 100 mW/cm^2 of the 12 μm thick film composed of P25 particles (dashed) or TiO_2 beads (solid) sensitized with the C101 dye without (in black color) and with $TiCl_4$ post-treatment (in red color).

TABLE 1. Cell Characteristics Recorded at 1 equiv Sunlight Intensity for 12 μm Thick Films Based on Degussa P25 Titania or Mesoporous Titania Beads before and after $TiCl_4$ Post-treatment[a]

	P25				beads			
	J_{sc} (mA/cm²)	V_{oc} (mV)	ff.	η (%)	J_{sc} (mA/cm²)	V_{oc} (mV)	ff.	η (%)
no post-treat.	12.27	756	0.754	7.1	16.50	735	0.742	9.1
$TiCl_4$ post-treat.	15.00	761	0.747	8.5	18.44	745	0.767	10.6

[a]The data corresponds to the best results over three cells. The cell's reproducibility was giving less than 0.2% discrepancy in PCE. ff. = fill factor.

significantly enhances the PCE through the augmentation of J_{sc} and V_{oc} at the expense of the fill factor.[15] In the case of the bead films, the $TiCl_4$ post-treatment remarkably improves the three characteristic cell parameters simultaneously; that is, the short circuit density increases notably from 16.5 to 18.4 mA/cm², the V_{oc} increases from 735 to 745 mV, and the fill factor increases from 0.74 to 0.77. The effect of this post-treatment is not completely understood to date. Nevertheless, results based on recombination rate and electron transport published by O'Regan *et al*. and further confirmed at the EPFL suggest a better charge collection efficiency subsequent to the post-treatment due to an increased electron lifetime with the carrier transport being only slightly affected.[15] The $TiCl_4$ coating may also improve connections between the relatively large beads in the film. In this study, application of the $TiCl_4$ post-treatment to the beads when using C101 leads to a PCE value as high as 10.6%, that is a 16.5% relative PCE enhancement compared to efficiencies measured on cells with no post-treatment.

For comparison, analogous films of similar thickness to the bead layer composed of Degussa P25 titania particles both before and after $TiCl_4$ post-treatment were likewise investigated. The cell characteristics for these two films are tabulated in Table 1. Strikingly, even without such a post-treatment, the utilization of the TiO_2 beads to prepare the electrode provides a significant advantage in terms of short circuit current density, leading to a jump of 2% in efficiency. This notable increase in photocurrent stems from the drastic enhancement of the external quantum efficiency (Figure 3a). In the presence of bead-shaped TiO_2 films the IPCE is superior over the entire range of light in which the C101 dye absorbs effectively. The IPCE attains a maximum of 92.1% at 570 nm indicating close to quantitative conversion of incident photons to electric current when taking into consideration the light losses ascribed to the TCO glass. By contrast the maximum IPCE of films produced with P25 particles was only 76.6% at the same wavelength. Such an enhancement is likewise maintained in the red region of the light, that is, 54% IPCE at 700 nm for the bead films *versus* 31.8% for the P25 films.

The superior optical characteristic of the beads is also clearly demonstrated when each IPCE maximum is normalized to 100% (Figure 3b). We can then visualize the strong impact of this new mesoporous-bead morphology on the conversion of lower photon energies with an important enhancement in light conversion efficiency from 600 nm until far in the absorption tail (to 800 nm). This improved light harvesting characteristic originates from the combination of an increased dye loading on the beads and on their higher diffusion reflectance properties, which attest to their superior light scattering properties.[10] It is surprising to find the PV characteristics of the DSC made from only a single titania layer composed of TiO_2 beads competes impressively with the achievement of 10.5% efficiency obtained on a two layered geometry composed of 9 μm thick transparent nanocrystalline TiO_2 + 5 μm 400 nm CCIC TiO_2 films (Supporting Information, Figure S2).

As the improvement in efficiency of DSCs composed of TiO_2 beads over Degussa P25 was also observed for

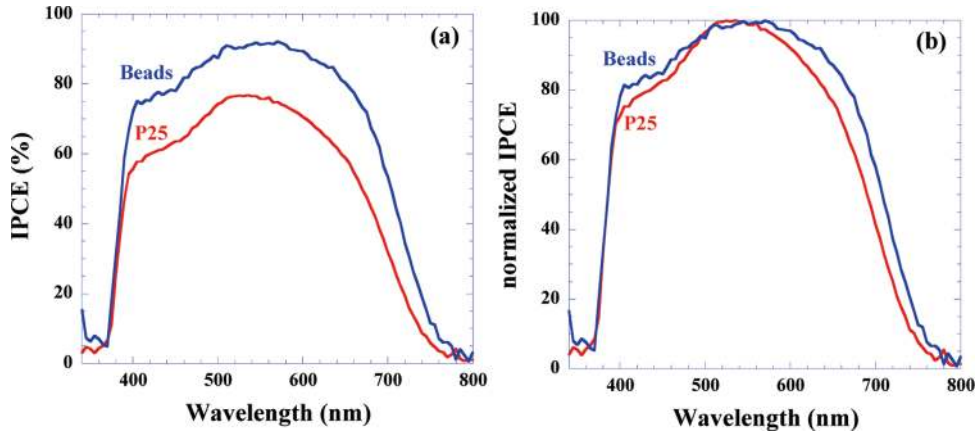

Figure 3. (a) IPCE spectrum of 12 μm thick films composed of P25 particles or mesoporous beads with $TiCl_4$ post-treatment sensitized with the C101 dye and (b) the normalized IPCE spectrum of titania beads and P25 titania particles.

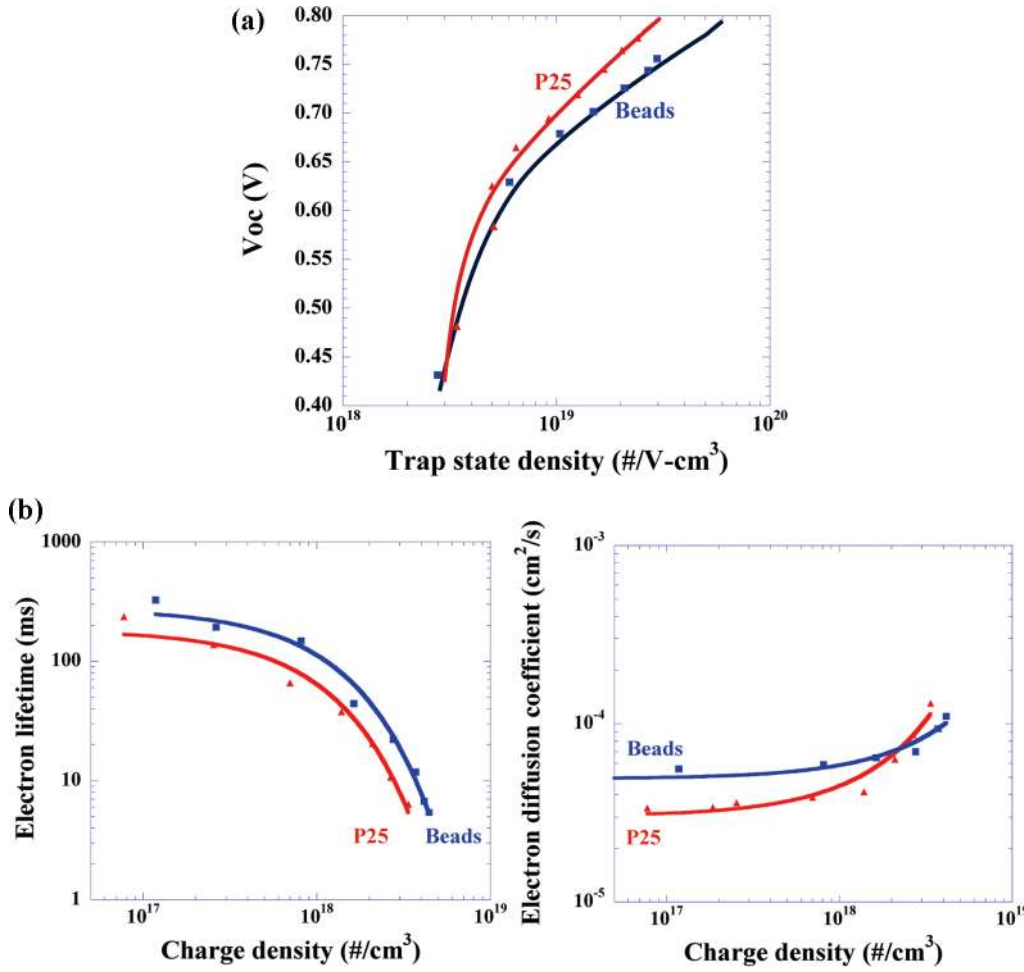

Figure 4. (a) Trap state distribution in P25 titania and bead films with $TiCl_4$ post-treatment. (b) Evolution of electron lifetime and electron diffusion coefficient as a function of charge density for P25 and beads with $TiCl_4$ post-treatment.

N719 dyed electrodes, with a substantial increase in short-circuit current,[10] the dynamics of charge transport and charge recombination were probed. Photovoltage and photocurrent transient techniques were employed to assess these dynamics. Figure 4a shows the single exponential trap states' distribution below the conduction band of TiO_2 for both P25 and bead containing films. The DOS (density of states) was derived from following the film capacitance evolution utilizing the so-called charge extraction technique.[16] When comparing the two films at a given trap density of 10^{19} charges/cm^3, for example, the trap states of the TiO_2 bead film are more deeply distributed within the forbidden band gap. This could be the origin of the lower V_{oc} when the titania beads were used. Using the rate constants derived from photovoltage and photocurrent decay measurements, the evolution of the electron lifetime (τ_n) and the electron diffusion coefficient (D_n) were both analyzed as a function of charge density (Figure 4b). For the entire range of charge densities evaluated, (that is, between *ca.* 10^{17} and 10^{19} charges/cm^3) the electron lifetime is observed to be superior, by two times, when utilizing the bead films indicating a slower electron recombination with the oxidized electrolyte species, I_3^-, in comparison to films composed of P25 particles.

The electron diffusion coefficient is likewise superior in bead films compared to P25 film layers at a charge density lower than *ca.* 2.1×10^{18} charges/cm^3. In the P25 electrode, there are many relatively large pores originating from the use of the binder during the film preparation resulting in less interconnects between particles. Therefore, electrons in the P25 electrode travel a longer path to the conducting substrate, resulting in a low diffusion coefficient. While in the bead electrode the TiO_2 nanocrystals are well interconnected within the beads, giving good electron transport. However, at a relatively high charge density, the devices containing bead-films start to exhibit a lower comparative electron diffusion coefficient underlining the narrow connection between the beads constraining the fast electron diffusion.

Using the values of the two parameters obtained from the photo transient techniques, the electron diffusion length was calculated as a function of charge density for the two types of particulate film, illustrated in Figure 5, following the formula $L_n = (D_n\tau_n)^{1/2}$.[16] An interconnected network of nanocrystalline spherical beads,

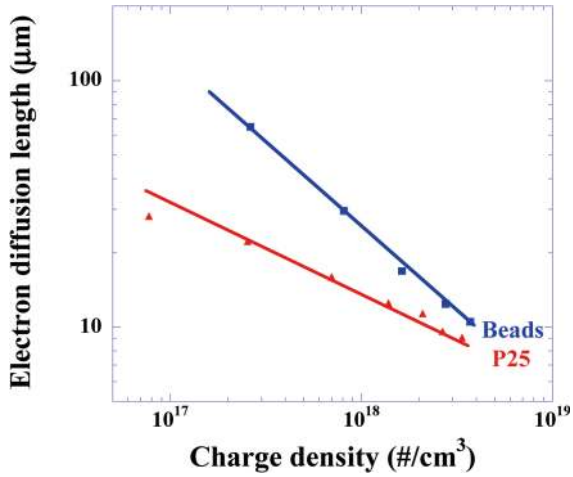

Figure 5. Evolution of the electron diffusion length for P25 titania and TiO_2 beads with $TiCl_4$ post-treatment.

as shown in Figure 1b−d, results in a longer electron diffusion length when compared to particulate films composed of P25, thus explaining the improved charge collection efficiency and higher photocurrent witnessed in the spherical bead photoanodes.

To summarize, the close packing of grains and crystal intergrowth within the mesoporous titania beads are believed to be responsible for the extended electron-lifetime in the films composed of beads, along with increased electron diffusion lengths. Combining these bead morphologies that give enhanced diffuse reflectance across the 600−800 nm wavelengths with dyes that absorb at lower energy than the standard N719 dye has resulted in a substantial enhancement in efficiencies. For the first time power conversion efficiencies surpassing the 10% level, that is, $\eta = 10.6\%$ under AM1.5G irradiation, exhibiting an IPCE of 92% at 570 nm, have been obtained using a single titania layer (12 μm thickness) composed of monodisperse spherical TiO_2 beads in conjunction with the heteroleptic thiophene-based dye, C101. Preliminary experiments show that significant improvement with PCE beyond 11.0% can be achieved employing a thin layer of transparent 20 nm-based particles between the TCO and the beads and sheltering the beads with a scattering layer (reported in Supporting Information Figure S3). The tuning of the size of the beads, their interconnections, and their pores to match with the opto-electronics of the C-dyes is now underway in order to bring DSC photovoltaic devices to a new level.

EXPERIMENTAL SECTION

Materials. All solvent and reagents were of *puriss* grade quality and were used as received. Guanidinium thiocyanate (GuNCS) and cheno-3a,7a-dihydroxy-5b-cholic acid were purchased from Fluka. 1,3-Dimethylimidazolium iodide (DMII) was prepared according to a reported procedure.[17] The purity was confirmed by ^{1}H NMR analysis.

Mesoporous Bead Synthesis. Amorphous precursor TiO_2 beads were synthesized using a sol−gel process in the presence of hexadecylamine.[10,11] A 1.6 g portion of air-dried precursor beads underwent solvothermal treatment in an ethanol−water mixture (2:1 by volume) containing 1.0 mL of 25 wt % ammonia solution, at 160 °C for 16 h. The solid products were collected by filtration, washed with ethanol, and dried in air at room temperature. Such solvothermally treated TiO_2 beads were used to prepare the screen-printing slurry for fabricating the TiO_2 films.

Device Fabrication. For the photoanode, single layer films of interconnected TiO_2 particles (either P25 or mesoporous beads) were screen-printed on FTO-type TCO glass through a 34T mesh-size screen. The films were sintered at 500 °C for 30 min before solar cell construction. A 300 μM portion of cheno-3a,7a-dihydroxy-5b-cholic acid was dissolved with an equimolar amount of C101 complex in a mixture of *tert*-butanol and acetonitrile solvent (1:1 by volume). After being washed by acetonitrile and dried in air, the overnight sensitized electrodes were sealed using a 25 μm thick Surlyn gasket, melted by heating with the Pt-modified TEC15 TCO counter-electrode. The latter was prepared by spreading out a drop of 5 mM H_2PtCl_6 ethanol solution onto the counter-electrode before treating it at 400 °C for 15 min under air. A hole was introduced in the counter-electrode by sand-blasting, allowing the internal space between the two electrodes to be filled with volatile Z960 electrolyte using a vacuum backfilling system, and then was sealed with a thin glass sheet. The Z960 electrolyte was composed of 1 M DMII, 50 mM LiI, 30 mM I_2, 0.5 M *tert*-butylpyridine, and 0.1 M GuNCS in a solvent mixture of 85% acetonitrile with 15% valeronitrile by volume.

The printed photoanode had a square geometry of 4 × 4 mm, and prior to measurements the cell was masked by a square black tape with a 0.125 cm^2 aperture. An antireflecting coating on the photoanode glass was also used to prevent reflection losses.

Photovoltaic and TiO_2 Characterization. A 450 W xenon light source (Oriel, USA) was used to provide an incident irradiance of 100 mW/cm^2 at the surface of the solar cells. The spectral output of the lamp was filtered using Schott K113 Tempax sunlight filter (Präzisions Glas & Optik GmbH, Germany) that enables light from 350 to 750 nm to pass through and hence to reduce light mismatch between real solar illumination and the simulated illumination to less than 2%. Light intensities were regulated with wire mesh attenuators. The (*J*−*V*) measurements were performed using a Keithley model 2400 digital source meter (Keithley, USA) by independently applying external voltage to the cell and by measuring the photogenerated current out from the cell. Incident photon-to-current conversion measurements were realized using a 300 W xenon light source (ILC Technology, USA). A Gemini-180 double monochromator Jobin Yvon Ltd. (UK), was used to select and increment wavelength radiation to the cell. The monochromatic incident light was passed through a chopper running at 1 Hz frequency and the on−off ratio was measured by an operational amplifier. This was superimposed on a constant white light bias corresponding to 50% solar intensity. The latter generates sufficient charge carrier concentration within the film to increase the collection rate of the electrons generated by the monochromatic light above the chopping frequency.

The film morphology was investigated using a high resolution scanning electron microscope FEI XL-30 SFEG coupled to a TLD (through the lens detector). The thickness of the electrode was determined by profilometry. The resulting mesoporous titania beads were ultramicrotomed to *ca.* 60 nm thickness to investigate the interior structure and crystal intergrowth on a FEI Tecnai F20 transmission electron microscope operating at 200 KV.

Acknowledgment. S.F., P.C., L.P.H., and M.G. wish to thank Aravind Kumar Chandiran, Dr. Shaik Zakeeruddin, Dr. Nicolas Te-

treault, Dr. Carole Graetzel, and Dr. Robin Humphry-Baker from LPI for fruitful discussion and acknowledge financial support of this work by the EU project "Robust DSC" grant agreement number 212792. D.C., F.H., Y.C., and R.A.C. acknowledge the Australian Research Council for financial support, and R.A.C. acknowledges an Australian Research Council Future Fellowship.

Supporting Information Available: The (*J*−*V*) characteristics for different light intensity (1 sun, 0.5 sun, and 0.1 sun) of (i) 12 μm thick film composed of TiO_2 beads sensitized with the N719 dye; (ii) 9 + 5 μm thick film composed of 20 nm-based TiO_2 particles sheltered by 400 nm CCIC particles sensitized with the C101 dye; (iii) 12 μm thick film composed of TiO_2 beads sensitized with the C106 dye; and (iv) a triple layer consisting of a first layer of 20 nm-based transparent electrode + mesoporous beads + CCIC scattering layer. This material is available free of charge *via* the Internet at http://pubs.acs.org.

REFERENCES AND NOTES

1. Fujishima, A.; Honda, K. Electrochemical Photolysis of Water at a Semiconductor Electrode. *Nature* **1972**, *238*, 37–39.
2. Grätzel, M. Materials Science—Ultrafast Colour Displays. *Nature* **2001**, *409*, 575–576.
3. Guo, Y. G.; Hu, Y. S.; Sigle, W.; Maier, J. Superior Electrode Performance of Nanostructured Mesoporous TiO_2 (Anatase) through Efficient Hierarchical Mixed Conducting Networks. *Adv. Mater.* **2007**, *19*, 2087–2091.
4. Gerischer, H. Neglected Problems in the pH-Dependence of the Flat-Band Potential of Semiconducting Oxides and Semiconductors Covered with Oxide Layers. *Electrochim. Acta* **1989**, *34*, 1005–1009.
5. Tien, T. Y.; Stadler, H. L.; Gibbons, E. F.; Zacmanidis, P. J. TiO_2 as an Air-to-Fuel Ratio Sensor for Automobile Exhausts. *Am. Ceram. Soc. Bull.* **1975**, *54*, 280–282.
6. O'Regan, B.; Grätzel, M. A Low-Cost, High-Efficiency Solar-Cell Based on Dye-Sensitized Colloidal TiO_2 Films. *Nature* **1991**, *353*, 737–740.
7. Feng, X. J.; Shankar, K.; Varghese, O. K.; Paulose, M.; Latempa, T. J.; Grimes, C. A. Vertically Aligned Single Crystal TiO_2 Nanowire Arrays Grown Directly on Transparent Conducting Oxide Coated Glass: Synthesis Details and Applications. *Nano Lett.* **2008**, *8*, 3781–3786.
8. Mor, G. K.; Shankar, K.; Paulose, M.; Varghese, O. K.; Grimes, C. A. Use of Highly-Ordered TiO_2 Nanotube Arrays in Dye-Sensitized Solar Cells. *Nano Lett.* **2006**, *6*, 215–218.
9. Lancelle-Beltran, E.; Prene, P.; Boscher, C.; Belleville, P.; Buvat, P.; Lambert, S.; Guillet, F.; Boissiere, C.; Grosso, D.; Sanchez, C. Nanostructured Hybrid Solar Cells Based on Self-Assembled Mesoporous Titania Thin Films. *Chem. Mater.* **2006**, *18*, 6152–6156.
10. Chen, D. H.; Huang, F. Z.; Cheng, Y. B.; Caruso, R. A. Mesoporous Anatase TiO_2 Beads with High Surface Areas and Controllable Pore Sizes: A Superior Candidate for High-Performance Dye-Sensitized Solar Cells. *Adv. Mater.* **2009**, *21*, 2206–2210.
11. Chen, D. H.; Cao, L.; Huang, F. Z.; Imperia, P.; Cheng, Y. B.; Caruso, R. A. Synthesis of Monodisperse Mesoporous Titania Beads with Controllable Diameter, High Surface Areas, and Variable Pore Diameters (14−23 nm). *J. Am. Chem. Soc.* **2010**, *132*, 4438–4444.
12. Van de Hulst, H. C. *Light Scattering by Small Particles*; Wiley: New York, 1957.
13. Gao, F.; Wang, Y.; Shi, D.; Zhang, J.; Wang, M. K.; Jing, X. Y.; Humphry-Baker, R.; Wang, P.; Zakeeruddin, S. M.; Grätzel, M. Enhance the Optical Absorptivity of Nanocrystalline TiO_2 Film with High Molar Extinction Coefficient Ruthenium Sensitizers for High Performance Dye-Sensitized Solar Cells. *J. Am. Chem. Soc.* **2008**, *130*, 10720–10728.
14. Cao, Y. M.; Bai, Y.; Yu, Q. J.; Cheng, Y. M.; Liu, S.; Shi, D.; Gao, F. F.; Wang, P. Dye-Sensitized Solar Cells with a High Absorptivity Ruthenium Sensitizer Featuring a 2-(Hexylthio)Thiophene Conjugated Bipyridine. *J. Phys. Chem. C* **2009**, *113*, 6290–6297.
15. O'Regan, B. C.; Durrant, J. R.; Sommeling, P. M.; Bakker, N. J. Influence of the $TiCl_4$ Treatment on Nanocrystalline TiO_2 Films in Dye-Sensitized Solar Cells. 2. Charge Density, Band Edge Shifts, and Quantification of Recombination Losses at Short Circuit. *J. Phys. Chem. C* **2007**, *111*, 14001–14010.
16. Wang, H. X.; Peter, L. A. A Comparison of Different Methods to Determine the Electron Diffusion Length in Dye-Sensitized Solar Cells. *J. Phys. Chem. C* **2009**, *113*, 18125–18133.
17. Bando, K. K.; Mitsuzuka, Y.; Sugino, M.; Sugihara, H.; Sayama, K.; Arakawa, H. Attachment of an Organic Dye on a TiO_2 Substrate in Supercritical CO_2: Application to a Solar Cell. *Chem. Lett.* **1999**, 853–854.